Layer-by-Layer Structure in Ultrathin Aniline and Pyridine Films on Ag(111)

M. C. Yang, T. J. Rockey, D. Pursell,† and H. L. Dai*

Department of Chemistry, University of Pennsylvania, Philadelphia, Pennsylvania 19104-6323

Received: August 20, 2001; In Final Form: October 8, 2001

Ultrathin (1−10 layers) aniline and pyridine films deposited on a Ag(111) surface at 90 K have been examined using thermal programmed desorption (TPD). Multiple desorption peaks have been observed for both systems showing film growth from the first chemisorbed layer to the bulk structure through multiple intermediate layers. The growth mechanisms for the two systems are, however, apparently different. Aniline films are formed one layer at a time with five thermodynamically stable layered structures. In contrast, pyridine films grow through metastable phases, similar to benzene film deposition on metal. In particular, a skin layer over the bulk phase is proposed to account for the TPD spectra. The difference in film growth mechanisms is attributed to the effect of intermolecular interactions.

The adsorption of organic molecules on surfaces and growth of corresponding thin films has been a topic of fundamental interest with practical implications in surface and materials sciences. Studies on molecular adsorption have revealed effects of adsorbate−substrate and interadsorbate interactions, which provide a basis for understanding growth and structure of molecular thin films. Still, how molecular and substrate properties affect thin-film structure and deposition remains to be explored.

Recently, notable advances have been made in organic thin-film semiconductor devices.[1−3] This development as well as those in nanotribology[4,5] have inspired the need for a fundamental understanding of the structure and growth of ultrathin molecular films. For example, a highly ordered, layered structure is crucial to achieving the performance of organic semiconductors.[3] In nanotribology, studies have shown that properties of ultrathin liquid films confined by two solid surfaces can be dramatically different from those of the bulk liquid.[4]

In general, the structure of a thin molecular film is determined by the nature of intermolecular interaction, molecular shape, substrate structure and adsorbate−substrate bonding, temperature, and even the deposition rate. Monatomic or diatomic model systems have been sought after for understanding the effect of these structural factors and testing analytical theories.[6] These systems, though sufficiently simple for theoretical treatment, may not reflect the diversity of structures and interactions in thin films of polyatomic molecules.

Benzene multilayers present a model system with higher complexity and richer observations.[7−9] Benzene, with high molecular symmetry and a disklike shape, allows a study of the effects of anisotropic intermolecular and molecule−substrate interactions. On most metal surfaces, benzene film deposition appears to go through a metastable structure from the first chemisorbed layer to the bulklike structure.[8]

The thin films of pyridine (C_5H_5N) and aniline ($C_6H_5NH_2$) may provide as further testing cases for comparison with benzene. Intermolecular interaction for pyridine is still weak but has added directionality. Aniline has a discernibly different shape from benzene. Moreover, hydrogen bonding is possible between aniline molecules. The adsorption of pyridine[10−12] and aniline[13−17] on metal surfaces has been studied before. None of these works, however, focused on the structure of the multilayers. In this report, we will show, through a temperature-programmed desorption (TPD) study, that different intermolecular interaction strength will result in dramatically different growth mechanisms and structures in ultrathin molecular films.

All experiments were performed in an UHV chamber (base pressure $\leq 2 \times 10^{-10}$ Torr). The Ag(111) surface was cleaned routinely by sputtering and annealing with its structure and impurities checked by LEED and EELS. Anhydrous aniline and pyridine (99.5%, Aldrich) were purified by several freeze−pump−thaw cycles before use. Gas molecules were introduced into the chamber by either a microcapillary array doser (13 mm diameter and 2 mm thickness with 50 μm diameter capillaries) or backfilling through a leak valve. The distance between the surface and the doser was 2.54 cm. The substrate temperature was kept at 90 K during deposition. TPD was performed with 1 K/s heating rate on samples prepared using both dosing methods. TPD peak positions and shapes were almost identical for both kinds of dosing methods, except that peak widths were broadened by 2 K when the doser was used. Because of the advantage of low background pressure increase, the doser was chosen for the aniline experiments where pumping residual gas was time-consuming. For pyridine samples, adjacent peaks in TPD spectra are within a few K of each other. As a result, backfilling, which generates sharper TPD peaks, was the preferred dosing method.

TPD spectra of aniline thin films prepared with increasing exposures at 90 K are shown in Figure 1. At lowest exposures, a broad feature, designated as α_1, appears near 260 K. Peak α_1 shifts to lower temperature and broadens with increasing exposure. After α_1 saturation in intensity, a second peak, α_2, starts to appear at 210 K. The peak area of α_1 at the saturation point is assigned as 1 ML for conversion from exposure to coverage. The third peak, α_3, at 187 K starts growing before α_2 is saturated. Notably, the maximum area of α_3 is less than 50% of that of α_1. A fourth peak, α_4, appears at 175 K whose

* To whom all correspondence should be addressed. Email: dai@sas.upenn.edu.

† Present address: Department of Chemistry, US Military Academy, West Point, NY 10996.

10.1021/jp013229p CCC: $20.00
Published on Web 11/06/2001

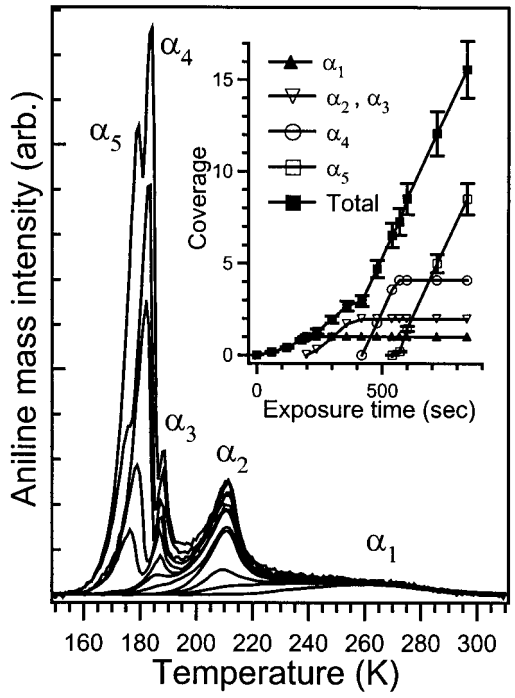

Figure 1. TPD of aniline deposited on Ag(111) at 90 K with increasing exposure. One monolayer (ML) is defined as the saturation coverage of peak α_1. Inset represents individual peak area of $\alpha_1-\alpha_5$ and total peak area in TPD spectra as a function of exposure time.

position shifts to higher temperature at higher coverage. Eventually, α_5 appears at 170 K after α_4 is saturated and continues to grow with exposure.

TPD of pyridine thin films shows dramatically different patterns, as seen in Figure 2a. A broad feature at 185 K, β_1, appears at lowest exposures. This feature at saturation also calibrates exposure to coverage. The second (β_2 at 144 K) and third (β_3 at 140 K) peaks appear in sequence with increasing exposure. In contrast to aniline, the last peak, β_4, appears at the expense of β_3. Most dramatically, the peak temperature of β_4 at 154 K is higher than both peaks β_2 and β_3!

The behavior of β_3 as a function of temperature and exposure is highly suggestive of a metastable phase, according to Polta et al.[7] To confirm this possibility, thermal stability of β_3 was examined by annealing experiments (Figure 2b). After annealing at 125 K for 2 min, a significant portion of β_3 was transformed into β_4, while there was no change in β_2. The aniline film annealing behavior, on the other hand, is quite different; no change in TPD spectra was observed for aniline films annealed for 3 min at 160, 180, and 195 K, before the onset of desorption for α_5, α_3 and α_2, respectively.

The shift to lower temperature with increasing exposure in α_1 is indicative of repulsive interaction between adsorbates.[18,19] The dipole−dipole repulsion model by Albano[19] was used to simulate the α_1 peak. A line-shape analysis yielded a desorption energy of 73.5 kJ/mol, assuming a preexponential factor of 1×10^{13} s^{-1}. The α_2 peak position is independent of coverage, showing first-order desorption kinetics.[18] Accordingly, desorption energy for α_2 was determined as 60.7 kJ/mol with a preexponential factor of 2×10^{14} s^{-1}. Line-shape analysis was not attempted for the small peak α_3. From the peak temperature, its desorption energy is estimated to be 7 kJ/mol lower than that of α_2. For α_4, the shift to higher temperature at higher coverage indicates the existence of attractive interactions among aniline molecules. A line-shape analysis using Bethe−Peierls model[18] yielded a 52.5 kJ/mol desorption energy and a preexponential factor of 7×10^{14} s^{-1} with a pair attractive interaction energy of 0.7 kJ/mol. Peak α_5 grows continuously with exposure, showing zero-order kinetics. An analysis of the leading-edge yielded a desorption energy of 52 ± 2 kJ/mol.

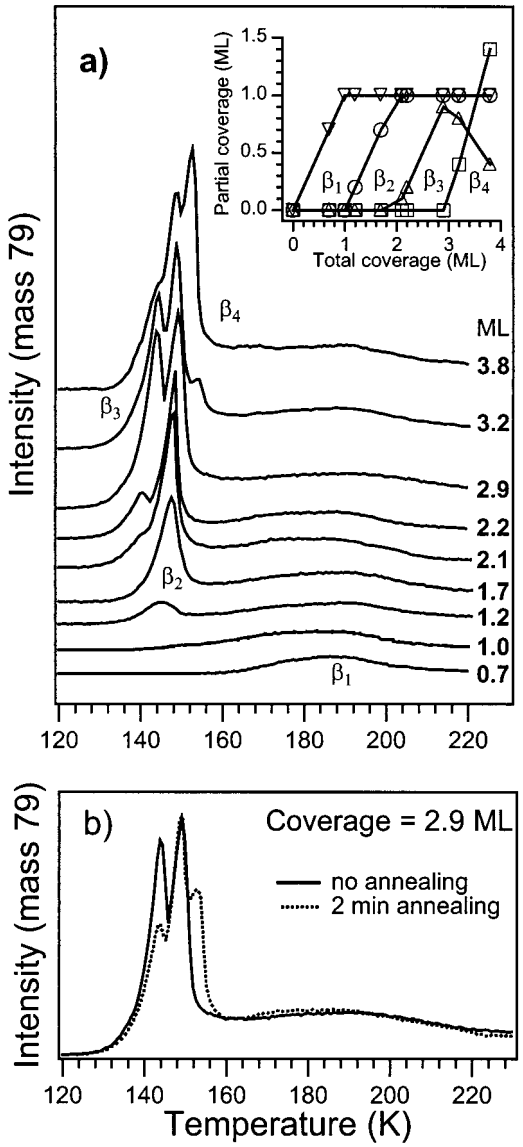

Figure 2. (a) TPD of pyridine deposited on Ag(111) at 90 K with increasing exposure. One monolayer (ML) is defined as the saturation coverage of peak β_1. Inset shows individual peak area of $\beta_1-\beta_4$ in TPD spectra as a function of total coverage. (b) TPD of pyridine films (2.9 ML) after annealing for 2 min. (····) and without annealing (—).

In the inset of Figure 1, the total and partial areas of aniline TPD peaks, converted into coverages, are plotted as a function of exposure time. The area of each peak was obtained from deconvolution using line-shapes determined from desorption energy analysis. The ratio of saturation coverages of $\alpha_1-\alpha_4$ is 1.0:1.5:0.5:4.1.

For pyridine TPD, full line-shape analyses cannot be reliably performed because of overlap of the peaks. However, an estimate of binding energy according to desorption temperature can be done assuming a preexponential factor of 1×10^{13} s^{-1}. Desorption energies of $\beta_1-\beta_3$ are 49.3, 37.7, and 36.6 kJ/mol, respectively. The peak β_4 continued growing with increasing exposure. A desorption energy of 48.3 ± 0.6 kJ/mol, much higher than those of β_2 and β_3, was obtained for β_4 from analyzing its leading-edge for a film with 30 ML of pyridine, where β_4 became dominant.

The coverage-exposure curve for pyridine films was not available because of uncertainty in exposure associated with the backfilling method. Instead, to visualize the relative intensity change of peaks $\beta_1-\beta_4$, partial coverage of each pyridine TPD peak was plotted with respect to total coverage in the inset of Figure 2a. Peaks β_2 and β_3 appear at the saturation point of β_1 and β_2, respectively. The last peak β_4 grows at the expense of β_3. The saturated intensities of β_1, β_2, and β_3 turn out to be about the same.

In previous observations of aromatic molecule adsorption on metal, such as benzene on Cu(111),[9] benzene on Ag(111),[20] and styrene on Pt,[21] the TPD peak of the first monolayer is broad and shifts toward lower temperature with exposure. The overlayers on top of the weakly chemisorbed[22] first layer desorb at lower temperatures with either first-order[9,21] or zero-order desorption kinetics.[20] Peaks α_1 and α_2 match the characteristics of the chemisorbed first layer and the overlayer and can be assigned accordingly. The surface has a nominal step concentration of <0.5%. The steps may contribute to the breadth of the TPD peak of the first monolayer but not to the lower-temperature peaks. As the last peak α_5 continues to grow with exposure, it is safe to assign it to a bulk aniline structure. The fact that $\alpha_1-\alpha_5$ appear in sequence of decreasing binding energy is consistent with the layer-by-layer growth from the bottom (first layer) to top (bulk). The ratio of the peak intensities reveals the density in individual layers. The peak α_1 at saturation represents a full monolayer of flat-lying aniline on Ag(111).[23] Peak α_2 is 1.5 times as intense as α_1 at saturation; perhaps the second layer has packed in 50% more molecules. Peak α_3, with one-third of the α_2 intensity, may arise from interstitial sites on the second overlayer. Peak α_4 may come from a layer 4 times denser than α_1 or more likely a double-layer structure with twice the density. Even without definitive structural information, the TPD results show that before growing into the bulk structure, aniline molecules go through four transitional, but thermodynamically stable, structures within the first several layers.

The lower aniline layers are more strongly bound and energetically more stable than the upper. Since all layers are in thermodynamic equilibrium, the upper layers must have higher entropy. This deduction is consistent with the observation that the growth rate, indicated by the slope of the curves in the inset of Figure 1, is higher for the upper layers (α_4 and α_5) than for the lower ($\alpha_1-\alpha_3$) under the same deposition conditions. In the higher layers with higher entropy, it is faster for an adsorbed molecule to accommodate into a less restricted orientation before desorption, thus, resulting in higher adsorption probability.

Peaks β_1 and β_2 of pyridine films can be similarly assigned to the first weakly chemisorbed layer and the first physisorbed overlayer, respectively. The similarity between the two systems, however, stops here. β_3 and β_4 do not appear in sequential temperatures. Furthermore, β_3 is thermodynamically unstable. Given that the intensities of β_1 and β_2 are the same and that β_4 grows at the expense of β_3, we propose the following mechanism for pyridine film growth.

The chemisorbed (β_1), first physisorbed (β_2) and metastable (β_3) layers are first formed sequentially. The intensity ratio of $\beta_1:\beta_2:\beta_3 = 1:1:1$ suggests that all three are single layers with about the same density. When additional pyridine molecules adsorb onto the second physisorbed layer (β_3), small 3-D clusters, which are energetically more stable than the 2-D metastable layer, begin to form. The 3-D clusters are formed due to intralayer diffusion of molecules allowed by weak intermolecular interactions and can be activated by annealing up to the desorption temperature. The 3-D nucleus may then continue to grow into the bulk phase (β_4).

The 2-D to 3-D transition has been suggested by Jakob and Menzel[24] for the justification of the metastable layer in benzene films on Ru(001). In this model, the metastable phase desorbs first, followed by the bulk phase, the first physisorbed and then the chemisorbed phase. This order of desorption peaks for benzene films, however, is not the same as the one observed here. For pyridine, the following differences are observed: The bulk phase, β_4, desorbs at a higher temperature than the first physisorbed phase, β_2! Furthermore, β_2 intensity, once it reaches saturation, remains always constant no matter what the film thickness is. Apparently, the benzene model needs to be refined for pyridine.

Following initial sequential deposition of β_1, β_2, and β_3, adsorption of additional molecules induces transformation of the layers (β_2 and β_3) with weaker interactions into the more tightly bound 3-D bulk phase β_4, which may consist of crystalline structures. As the crystalline phase grows, a skin layer is developed. The skin layer has been suggested to appear in crystalline formation of atoms or molecules with weak interatomic interactions.[8,25] The skin layer is likely to have binding energy similar to that of the physisorbed overlayer and therefore desorbs at β_2. The apparent TPD sequence would be first β_2, followed by β_4 and β_1.

Why does aniline form stable layer-by-layer structures while pyridine and benzene undergo metastable to stable phase transitions? The driving force of this phase transition is the free energy difference that relates to intermolecular potentials and molecular orientation. The rate of transition depends on molecular diffusion, also determined by intermolecular interactions. Considering the three systems, the most apparent differences are in intermolecular interactions and molecular shapes; both pyridine and benzene have similar molecular shape and van der Waals intermolecular interactions, while aniline has a somewhat different shape with stronger intermolecular interaction through hydrogen bonding. The role of the shape may not be revealed without detailed structural information. One can speculate, however, that stronger interaction among aniline molecules allows them to form thermodynamically more stable structures and, thus, prevents their diffusion to form 3-D islands.

The role of intermolecular potential in thin-film properties is further supported by a comparison of the desorption temperatures of pyridine and benzene films. It is significant that the peak temperatures of the bulk phases of the two systems are nearly identical: 153 K for pyridine and 152 K for benzene on Ru(001). This is consistent with the fact that the lattice energies[26] are nearly the same for pyridine (−50.9 kJ/mol) and benzene (−52.3 kJ/mol). The peak temperatures of the two metastable phases (140 and 142 K) are also nearly the same.

Acknowledgment. This work is supported in part by a grant from the Air Force Office of Scientific Research. The equipment is supported by the National Science Foundation, MRSEC program, Grant No. DMR00-79909.

References and Notes

(1) Forrest, S. R. *Chem. Rev.* **1997**, *97*, 1793.
(2) Schoonveld, W. A.; Wildeman, J.; Fichou, D.; Bobbert, P. A.; van Wees, B. J.; Klapwijk, T. M. *Nature* **2000**, *404*, 977.
(3) Dodabalapur, A.; Torsi, L.; Katz, H. E. *Science* **1995**, *268*, 270.
(4) In *Handbook of Micro/nano Technology*, 2nd ed.; Bhushan, B., Ed.; CRC Press: Boca Raton, 1999.
(5) Bhushan, B.; Israelachvili, J. N.; Landman, U. *Nature* **1995**, *374*, 607.
(6) Marx, D.; Wiechert, H. *Adv. Chem. Phys.* **1996**, *95*, 213.

(7) Polta, J. A.; Thiel, P. A. *J. Am. Chem. Soc.* **1986**, *108*, 7560.
(8) Jakob, P.; Menzel, D. *J. Chem. Phys.* **1996**, *105*, 3838.
(9) Xi, M.; Yang, M. X.; Jo, S. K.; Bent, B. E.; Stevens, P. *J. Chem. Phys.* **1994**, *101*, 9122.
(10) Demuth, J. E.; Christmann, K.; Sanda, P. N. *Chem. Phys. Lett.* **1980**, *76*, 201.
(11) Haq, S.; King, D. A. *J. Phys. Chem.* **1996**, *100*, 16957.
(12) Lee, J.-G.; Ahner, J.; Yate, J. T., Jr. *J. Chem. Phys.* **2001**, *114*, 1414.
(13) Lee, K. K.; Vohs, J. M.; DiNardo, N. J. *Synth. Met.* **2000**, *113*, 231.
(14) Plank, R. V.; DiNardo, N. J.; Vohs, J. M. *Phys. Rev. B.* **1997**, *55*, 10241.
(15) Solomon, J. L.; Madix, R. J.; Stohr, J. *Surf. Sci.* **1991**, *255*, 12.
(16) Ramsey, M. G.; Rosina, G.; Steinmuller, D.; Graen, H. H.; Netzer, F. P. *Surf. Sci.* **1990**, *232*, 266.
(17) Schoofs, G. R.; Benziger, J. B. *J. Phys. Chem.* **1988**, *92*, 741.
(18) Masel, R. I. *Principles of Adsorption and Reaction on Solid Surfaces*; John Wiley & Sons: New York, 1996.
(19) Albano, E. V. *J. Chem. Phys.* **1986**, *85*, 1044.
(20) Zhou, X. L.; Castro, M. E.; White, J. M. *Surf. Sci.* **1990**, *238*, 215.
(21) Bai, J.; Snively, C. M.; Delgass, W. N.; Lauterbach, J. *Macromolecules* **2001**, *34*, 1214.
(22) The molecule-Ag bonding is characterized here as weakly chemisorbed following the convention established for these systems in Avouris, P.; Demuth, J. E. *J. Chem. Phys*. **1981**, *75*, 4783.
(23) Rockey, T.; Yang, M. C.; Lee, K. K.; Vohs, J. M.; Dai, H. L. To be sumitted to *Surf. Sci.*
(24) Jakob, P.; Menzel, D. *Surf. Sci.* **1989**, *220*, 70.
(25) Pluis, B.; Frenkel, D.; Vanderveen, J. F. *Surf. Sci.* **1990**, *239*, 282.
(26) Price, S. L.; Stone, A. J. *Mol. Phys.* **1984**, *51*, 569.